

High-Pressure Stopped-Flow Study of the Complexation of Vanadium(II) with Thiocyanate in Water: Further Evidence for the Associative Character of Substitution on This Metal Ion

PETER J. NICHOLS, YVES DUCOMMUN, and ANDRÉ E. MERBACH*

Received March 22, 1983

A high-pressure stopped-flow spectrophotometer has been built and used to study the substitution of thiocyanate onto hexaaquovanadium(II) in acidic aqueous solution. The kinetic parameters obtained are $k_f^{298} = 24.0 \pm 0.9 \text{ M}^{-1} \text{ s}^{-1}$, $\Delta H_f^* = 66.6 \pm 1.6 \text{ kJ mol}^{-1}$, $\Delta S_f^* = 4.9 \pm 5.4 \text{ J K}^{-1} \text{ mol}^{-1}$, and $\Delta V_f^* = -2.1 \pm 0.8 \text{ cm}^3 \text{ mol}^{-1}$ for the forward reaction and $k_r^{298} = 0.92 \pm 0.05 \text{ s}^{-1}$, $\Delta H_r^* = 62.7 \pm 2.6 \text{ kJ mol}^{-1}$, $\Delta S_r^* = -35.0 \pm 9.4 \text{ J K}^{-1} \text{ mol}^{-1}$, and $\Delta V_r^* = -11.5 \pm 0.9 \text{ cm}^3 \text{ mol}^{-1}$ for the reverse reaction. The activation parameters for the interchange step of SCN^- complexation are found to be similar to those for the water exchange on $\text{V}(\text{H}_2\text{O})_6^{2+}$ as obtained previously by NMR techniques. The activation volumes for the two processes are consistent with an associative interchange (I_a) of ligands.

Introduction

The exchange of water on $\text{V}(\text{H}_2\text{O})_6^{2+}$ in aqueous solution occurs via an associative interchange (I_a) mechanism as characterized by its negative volume of activation, $\Delta V_{\text{ex}}^* = -4.1 \pm 0.1 \text{ cm}^3 \text{ mol}^{-1}$.¹ This departure from the previously accepted dissociative interchange (I_d) process² is but part of a general trend in behavior for solvent exchange on the divalent ions of the first transition-metal series.³⁻⁶ Ligand substitution reactions on these metal ions have only been extensively studied for nickel(II) and cobalt(II). For these two ions, the same dissociative interchange mechanisms found for solvent exchange also operate for the complex formation reactions.⁵ This work was undertaken to test whether the associative interchange found for water exchange on $\text{V}(\text{H}_2\text{O})_6^{2+}$ is also the general mechanism for complex formation with this ion.

Experimental Section

The solutions were prepared at room temperature with deionized water. VCl_2 solutions were prepared by reduction of acidified (HCl, Merck, p.a.) VCl_3 (Fluka, p.a.) over a Zn/Hg amalgam under inert atmosphere.¹ For the variable-temperature work, the reduction was carried out on the stopped-flow apparatus itself, whereas for the high-pressure measurements the reservoir syringes were filled under nitrogen in a glovebox. Potentiometric titration against bromate⁷ showed that all the vanadium(III) was converted to vanadium(II). At the Cl^- concentration used, it had been previously checked that no chloride complexes are formed.¹ KSCN (Merck, p.a.) was used as received. Ionic strength was adjusted to 0.5 M with LiCl or LiClO_4 (Fluka, p.a.). Solutions were prepared volumetrically and concentrations expressed in molarity (M) at 0.1 MPa. No correction was made for variations in solution volumes with pressure and temperature.⁸ A Perkin-Elmer Hitachi 340 spectrophotometer with thermostated cells was used for equilibrium studies and routine checking of solutions.

Both the conventional and high-pressure stopped-flow spectrophotometers used the same optical and data collection/analysis arrangements. Optical fibers guided light from a stabilized 50-W quartz halogen lamp through a Hi-Tech MG/10 grating monochromator to a Hamamatsu R928 photomultiplier for single-wavelength measurements and through a Jarrell-Ash spectrograph to a Tracor Northern 1223 diode array detector for simultaneous multiwavelength spectra accumulation. A Tracor Northern 1710 modular signal

analyzer collected and analyzed the kinetic data.

For the variable-temperature work, a commercial Hi-Tech SFL-40 stopped-flow module was used, whereas for variable-pressure work a high-pressure apparatus was built. As with the instruments previously built by Heremans et al. and Kelm et al.,⁹ it consists of a high-pressure bomb containing the stopped-flow module. The pressure bomb is an AISI 316L stainless-steel cylinder (40-mm inner diameter) supporting pressure up to 200 MPa, topped by a stainless-steel plate and a beryllium-copper cap, arranged in a flat Bridgeman seal. The syringe drive (4-mm diameter steel rod) passes through the center of the plate, through a PTFE seal. Two sapphire windows, imbedded in reverse Bridgeman seals are aligned on each side of the cylinder. The pressure is transmitted via a connector at the bottom of the bomb and measured outside the bomb with a calibrated piezoelectric transducer (Novaswiss). Thermostating is ensured by the circulation of a fluid through a helical serpentine drilled in the bomb wall. The temperature is measured at window level by a 100- Ω resistor placed in the bomb, on the wall.¹⁰

The inner stopped-flow unit is made of CTFE. The mixing cell (1-cm path length, 0.2-cm diameter) and the inlet and outlet capillaries are drilled in a single block, on which the two injection syringes and the receiving syringe are screwed. A sapphire window is placed at each end of the observation path, held in place by a stainless-steel nut.

In the instruments of Heremans and Kelm, the syringe drive unit was placed inside the pressure bomb. In our instrument, the injection is accomplished by sliding a finite length of the rod through the top of the pressure bomb by means of a pneumatic drive shot. Since the inside free volume of the bomb is 200 cm^3 , the pressure increase due to penetration of the rod is negligible (<0.2 MPa/injection). The system allows variation of the injection volume (typically 80 μL) and a maximum of 40 injections without refilling the syringes. The dead time was calculated to be 4 ms, but 15 ms is required for complete mixing.

Results

The rate of reaction of $\text{V}(\text{H}_2\text{O})_6^{2+}$ with SCN^- was measured with a large excess of metal ($\geq 5:1$ metal to ligand ratio), to ensure pseudo-first-order kinetics and monocomplex formation. The reaction was found to follow first-order kinetics for longer than 3 half-lives, and the observed rate constants, k_{obsd} , were independent of the wavelength of observation (310–800 nm). VCl_2 solutions exposed to atmospheric oxygen gave rise to increased reaction rates due to the presence of vanadium species of higher oxidation state. Varying the concentration of acid from 10^{-3} to 10^{-1} M produced no significant variation in the measured rate constants. Plots of k_{obsd} against $[\text{V}(\text{H}_2\text{O})_6^{2+}]$ at constant ionic strength, temperature, and pressure were linear with nonzero intercepts (Figure 1). These observations are in agreement with previous studies of this

(1) Ducommun, Y.; Zbinden, D.; Merbach, A. E. *Helv. Chim. Acta* **1982**, *65*, 1385.

(2) Burgess, J. "Metal Ions in Solution"; Ellis Horwood: Chichester, England, 1978; Chapters 11 and 12.

(3) Ducommun, Y.; Newman, K. E.; Merbach, A. E. *Helv. Chim. Acta* **1979**, *62*, 2511.

(4) Meyer, F. K.; Newman, K. E.; Merbach, A. E. *J. Am. Chem. Soc.* **1979**, *101*, 5588.

(5) Ducommun, Y.; Newman, K. E.; Merbach, A. E. *Inorg. Chem.* **1980**, *19*, 3696.

(6) Merbach, A. E. *Pure Appl. Chem.* **1982**, *54*, 1479.

(7) Erdey, L.; Mázor, L. *Acta Chim. Acad. Sci. Hung.* **1953**, *3*, 469.

(8) Isaacs, N. S. "Liquid Phase High Pressure Chemistry"; Wiley: Chichester, England, 1981; p 186.

(9) (a) Heremans, K.; Snauwaert, J.; Rijkenberg, J. *Rev. Sci. Instrum.* **1980**, *51*, 806. (b) van Eldik, R.; Palmer, D. A.; Schmidt, R.; Kelm, H. *Inorg. Chim. Acta* **1981**, *50*, 131.

(10) Meyer, F. K.; Merbach, A. E. *J. Phys. E* **1979**, *12*, 185.

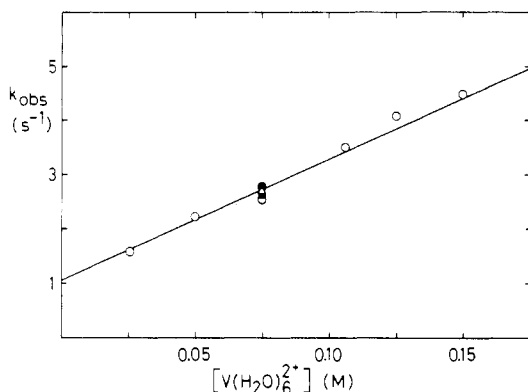


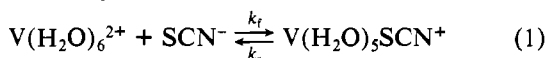
Figure 1. First-order rate constants, k_{obs} , as a function of $[\text{V}(\text{H}_2\text{O})_6^{2+}]$ at 298.2 K (ionic strength 0.5 M (LiClO_4); $[\text{SCN}^-] = 0.0025\text{--}0.01$ M; wavelength of observation 320 nm): ●, 0.001 M in H^+ ; △, 0.01 M in H^+ ; ○, 0.05 M in H^+ ; ■, 0.1 M in H^+ .

Table I. Rate and Equilibrium Constants for the Reaction between $\text{V}(\text{H}_2\text{O})_6^{2+}$ and SCN^- at Different Temperatures

T , K	k_f^a , $\text{M}^{-1} \text{s}^{-1}$	k_r^a , s^{-1}	log K	
			kinetics ^a	spectro-photometry ^{b,c}
274.1	2.26 ± 0.34	0.082 ± 0.022	1.43 ± 0.19	
283.2	5.71 ± 0.27	0.221 ± 0.017	1.41 ± 0.05	
293.2	13.8 ± 0.9	0.656 ± 0.062	1.32 ± 0.08	
298.2	22.3 ± 1.3	1.06 ± 0.09	1.32 ± 0.05	1.43 ± 0.11
303.2	41.8 ± 3.1	1.07 ± 0.23	1.59 ± 0.13	
313.2	96.2 ± 4.4	3.24 ± 0.30	1.48 ± 0.06	
323.2	193 ± 20	6.10 ± 1.37	1.51 ± 0.15	1.15 ± 0.20

^a Ionic strength 0.5 M (LiClO_4); wavelength of observation 320 nm; $[\text{V}(\text{H}_2\text{O})_6^{2+}] = 0.025\text{--}0.15$ M; $[\text{SCN}^-] = 0.0025\text{--}0.01$ M; $[\text{H}^+] = 0.001\text{--}0.1$ M (mostly 0.05 M). ^b Reference 15. ^c Ionic strength 0.5 M (LiCl); wavelength of observation 770 nm; $[\text{V}(\text{H}_2\text{O})_6^{2+}] = 0.015\text{--}0.15$ M; $[\text{SCN}^-] = 0.005\text{--}0.01$ M; $[\text{H}^+] = 0.05$ M.

system.¹¹⁻¹³ The results are consistent with reversible reaction kinetics as expressed by eq 1 and 2. The forward and reverse rate constants, k_f and k_r , were determined from weighted linear least-squares analysis.¹⁴



$$k_{\text{obsd}} = k_f[\text{V}(\text{H}_2\text{O})_6^{2+}] + k_r \quad (2)$$

Reaction 1 was studied as a function of temperature (274.0–323.1 K) and pressure (0.1–160 MPa). Table I lists the calculated k_f and k_r values at various temperatures. Weighted least-squares fitting¹⁴ of the data to the Eyring equation yielded $\Delta H_f^* = 66.6 \pm 1.6$ kJ mol⁻¹ and $\Delta S_f^* = 4.9 \pm 5.4$ J K⁻¹ mol⁻¹ for the forward reaction and $\Delta H_r^* = 62.7$

(11) Malin, J. M.; Swinehart, J. H. *Inorg. Chem.* **1968**, *7*, 250.

(12) Kruse, W.; Thusius, D. *Inorg. Chem.* **1968**, *7*, 464.

(13) Baker, B. R.; Sutin, N., unpublished observations (cited in: Baker, B. R.; Orhanovic, M.; Sutin, N. *J. Am. Chem. Soc.* **1967**, *89*, 722).

(14) For the calculation of k_f and k_r , the weighting applied to k_{obsd} values was $1/(k_{\text{obsd}})^2$ and is applicable for a constant relative error on each measurement. For the calculation of the activation parameters, the weighting factors were set equal to the inverse square of the calculated standard deviations on k_f and k_r . Error limits given throughout the text and tables are the standard deviations obtained from the least-squares treatments.

(15) Equilibrium constants were evaluated from the following equation: $C_{\text{LO}}/(A - \epsilon_V C_{\text{VO}}) = 1/KC_V(\epsilon_{\text{VL}} - \epsilon_V) + 1/(\epsilon_{\text{VL}} - \epsilon_V)$, where C_{LO} and C_{VO} are the total concentrations of SCN^- and $\text{V}(\text{II})$, respectively, C_V is the equilibrium concentration of $\text{V}(\text{H}_2\text{O})_6^{2+}$, A is the absorbance at 770 nm, and ϵ_V and ϵ_{VL} are the extinction coefficients for $\text{V}(\text{H}_2\text{O})_6^{2+}$ and $\text{V}(\text{H}_2\text{O})_5\text{SCN}^+$ at 770 nm. SCN^- does not absorb in this region while $\epsilon_V = 2$ M⁻¹ cm⁻¹ and $\epsilon_{\text{VL}} = 10$ M⁻¹ cm⁻¹ at 298.2 K. The K and ϵ_{VL} values were determined by a linear least-squares analysis using C_{VO} as estimates for C_V . With use of this K value, better estimates for C_V were obtained and used to recalculate K and ϵ_{VL} . After four such cycles, K and ϵ_{VL} were constant.

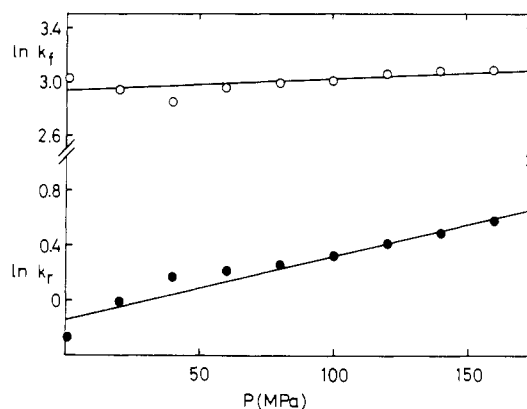


Figure 2. Effect of pressure on the forward and reverse rate constants at 298.2 K.¹⁶

Table II. Comparison of Water Exchange and SCN^- Interchange Parameters for $\text{V}(\text{H}_2\text{O})_6^{2+}$

	k^{298} , s^{-1}	ΔH^* , kJ mol^{-1}	ΔS^* , $\text{J K}^{-1} \text{mol}^{-1}$	ΔV^* , $\text{cm}^3 \text{mol}^{-1}$
water exchange ^a	87 ± 4	61.8 ± 0.7	-0.4 ± 1.9	-4.1 ± 0.1
SCN^- interchange ^b	20 ± 1	65.7 ± 1.6	0.6 ± 5.4	-5.3 ± 0.8

^a Reference 1. ^b Outer-sphere equilibrium data calculated by using the equations of Fuoss¹⁷ and Hemmes¹⁸ with ionic strength 0.5 M and distance of closest approach, a , 0.5 nm. $K_{\text{os}}^{298} = 1.2$ M⁻¹, $\Delta H_{\text{os}}^0 = +0.9$ kJ mol⁻¹, $\Delta S_{\text{os}}^0 = +4.3$ J K⁻¹ mol⁻¹, and $\Delta V_{\text{os}}^0 = +3.2$ cm³ mol⁻¹. $k_{\text{I}} = k_f/K_{\text{os}}$, $\Delta H_{\text{I}}^* = \Delta H_f^* - \Delta H_{\text{os}}^0$, $\Delta S_{\text{I}}^* = \Delta S_f^* - \Delta S_{\text{os}}^0$, and $\Delta V_{\text{I}}^* = \Delta V_f^* - \Delta V_{\text{os}}^0$.

± 2.6 kJ mol⁻¹ and $\Delta S_r^* = -35.0 \pm 9.4$ J K⁻¹ mol⁻¹ for the reverse reaction. These values differ from those obtained by Malin and Swinehart¹¹ ($\Delta H_f^* = 56.5 \pm 3.3$ kJ mol⁻¹ and $\Delta S_f^* = -29 \pm 17$ J K⁻¹ mol⁻¹; $\Delta H_r^* = 78.2$ kJ mol⁻¹ and $\Delta S_r^* = 37.7$ J K⁻¹ mol⁻¹), but their earlier work involved a smaller temperature range (278.6–310.1 K) and a different ionic strength (0.84 M). Our values for the forward and reverse rate constants obtained from the Eyring plots at 298.2 K are $k_f = 24.0 \pm 1.0$ M⁻¹ s⁻¹ and $k_r = 0.92 \pm 0.05$ s⁻¹, which is in the range of the previously reported values ($k_f = 28 \pm 3$,¹¹ 15 ± 2 ,¹² and 9 ± 1 M⁻¹ s⁻¹;¹³ $k_r = 1.0$ s⁻¹¹¹ and 1.4 ± 0.2 s⁻¹¹²).

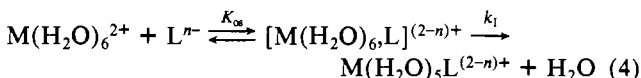
The variation of $\ln k_f$ and $\ln k_r$ with pressure at 298.2 K¹⁶ is shown in Figure 2. The results were fitted to eq 3 with k_0 ,

$$\ln k = \ln k_0 - \frac{\Delta V^*}{RT} P \quad (3)$$

the rate constant at zero pressure, and ΔV^* , the pressure-in-dependent volume of activation, as parameters. The rate constants at zero pressure are $k_{f,0} = 18.7 \pm 0.6$ M⁻¹ s⁻¹ and $k_{r,0} = 0.87 \pm 0.03$ s⁻¹, similar to those found independently in the variable-temperature study. The volumes of activation are $\Delta V_f^* = -2.1 \pm 0.8$ cm³ mol⁻¹ and $\Delta V_r^* = -11.5 \pm 0.9$ cm³ mol⁻¹. From these values the volume of reaction ($\Delta V^0 = \Delta V_f^* - \Delta V_r^*$) is calculated to be $+9.4$ cm³/mol⁻¹.

Discussion

The replacement of a water molecule of an aquated divalent transition-metal ion by a ligand is usually described by the Eigen-Wilkins mechanism. It involves the formation of an outer-sphere complex followed by the slow interchange of a bound water molecule for the ligand as shown in eq 4.² The



(16) $T = 298.2$ K; ionic strength 0.5 M (LiCl); wavelength of observation 770 nm; four to six solutions of different compositions at each pressure (k_{obsd} is the average of six to ten runs); $[\text{V}(\text{H}_2\text{O})_6^{2+}] = 0.025\text{--}0.15$ M; $[\text{SCN}^-] = 0.005\text{--}0.01$ M.

Table III. Volumes of Activation, ΔV_1^* ,^a for the Interchange of Ligands on Divalent Metal Ions in Aqueous Solution

ligand	V ²⁺	Mn ²⁺	Fe ²⁺	Co ²⁺	Ni ²⁺	Cu ²⁺	Zn ²⁺	ref
H ₂ O	-4.1 ± 0.1	-5.4 ± 0.1	+3.8 ± 0.2	+6.1 ± 0.2	+7.2 ± 0.3			1, 5
NH ₃				+4.8 ± 0.7	+6.0 ± 0.3			20
imidazole					+11.0 ± 1.6			21
isoquinoline					+7.2 ± 1.6			22
PADA ^b				+7.2 ± 0.2	+7.7 ± 0.3			20
				+11.2 ± 2.5	+8.2 ± 2.1			23
bpy ^c		-1.2 ± 0.2						19
SCN ⁻	-5.3 ± 0.8							this work
glycinate(1-)				+5 ± 2	+7 ± 1	+9 ± 1	+4 ± 1	24
murexide(1-)					+8.7 ± 1.5			25
malonate(2-)					+8.7 ± 2.1			26

^a In cm³ mol⁻¹; $\Delta V_1^* = \Delta V_f^* - \Delta V_{os}^0$; $\Delta V_{os}^0 = 0$ for neutral ligands, $\Delta V_{os}^0 = +3.2$ cm³ mol⁻¹ for uninegative ligands,²⁴ and $\Delta V_{os}^0 = +7.3$ cm³ mol⁻¹ for dinegative ligands.²⁶ ^b Pyridine-2-azo-(*p*-dimethylaniline). ^c 2,2'-Bipyridine.

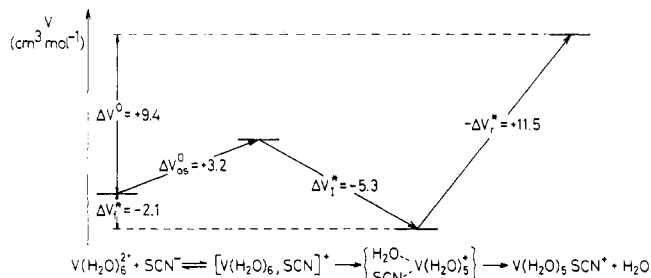


Figure 3. Volume profile for the formation of pentaquo(thiocyanato)vanadium(II).

formation of the outer-sphere complex is generally not observable, and the overall reaction appears second order. The forward rate constant k_f can then be expressed by eq 5. The

$$k_f = K_{os}k_1 \quad (5)$$

preequilibrium constant, K_{os} , and the volume of reaction, ΔV_{os}^0 , can be estimated from electrostatic models^{17,18} and hence the rate constant, k_1 , and activation parameters for the interchange step evaluated. They can now be compared to the corresponding parameters for water exchange on the metal ion as shown in Table II for the reaction between V(H₂O)₆²⁺ and SCN⁻.

The volume of activation for the interchange step, ΔV_1^* , is clearly negative as is the value found for the water exchange. This indicates a compressed transition state that can only result from a predominantly bond-making process, i.e. an associatively activated mechanism. Figure 3 depicts the volume profile for the substitution reaction. An initial volume increase occurs due to electrostriction changes on forming the outer-sphere complex. It is then followed by the compression of the system on bond formation to reach the transition state. The

final release of water produces a large expansion of the system, which is responsible for the overall positive volume of reaction.

A negative volume of activation has also been reported for the reaction of 2,2'-bipyridine with Mn(H₂O)₆²⁺,¹⁹ the other ion of the series for which a negative ΔV_{ex}^* is found for the water exchange.⁵ Table III summarizes all the results obtained from variable-pressure studies of divalent metal ion substitution reactions. As previously detailed¹ for solvent exchange, there exists a changeover in mechanism from I_a to I_d on going along the series from V(II) to Ni(II). A similar trend seems to be emerging from these ligand substitution studies. Future work is aimed at confirming that such a changeover is the general rule for the substitution reactions of octahedral transition-metal ions.

Acknowledgment. The authors express their thanks to R. Ith, P. Pollien, and R. Tschanz for their machine work in the construction of the high-pressure stopped-flow spectrophotometer and for their valuable suggestions regarding design. They also thank Prof. H. Kelm and Dr. R. van Eldik for helpful discussions. The Herbette Foundation and the Swiss National Science Foundation (Grant 2.256-0-81) are thanked for financial support.

Registry No. V(H₂O)₆²⁺, 15696-18-1; SCN⁻, 302-04-5.

Supplementary Material Available: The measured first-order rate constants (Tables SI and SII), the second-order forward and first-order reverse rate constants at various pressures (Table SIII), and the absorbances of V(H₂O)₆²⁺/SCN⁻ solutions (Table SIV) (4 pages). Ordering information is given on any current masthead page.

(17) Fuoss, R. M. *J. Am. Chem. Soc.* **1958**, *80*, 5059.
 (18) Hemmes, P. *J. Phys. Chem.* **1972**, *76*, 895.

(19) Doss, R.; van Eldik, R. *Inorg. Chem.* **1982**, *21*, 4108.
 (20) Caldin, E. F.; Grant, M. W.; Hasinoff, B. B. *J. Chem. Soc., Faraday Trans. 1* **1972**, *68*, 2247.
 (21) Yu, A. D.; Waissbluth, M. D.; Grieger, R. A. *Rev. Sci. Instrum.* **1973**, *44*, 1390.
 (22) Ishihara, K.; Funahashi, S.; Tanaka, M. *Inorg. Chem.* **1983**, *22*, 2070.
 (23) Caldin, E. F.; Greenwood, R. C. *J. Chem. Soc., Faraday Trans. 1* **1981**, *77*, 773.
 (24) Grant, M. W. *J. Chem. Soc., Faraday Trans. 1* **1973**, *69*, 560.
 (25) Jost, A. *Ber. Bunsenges. Phys. Chem.* **1975**, *79*, 850.
 (26) Inoue, T.; Kojima, K.; Shimozawa, R. *Chem. Lett.* **1981**, 259.